Phases of $(2+1)$D SO(5) Nonlinear Sigma Model with a Topological Term on a Sphere: Multicritical Point and Disorder Phase

Bin-Bin Chen[ ],[1] Xu Zhang,[1] Yuxuan Wang,[2,*] Kai Sun,[3,†] and Zi Yang Meng[ ][1,‡]

[1]*Department of Physics and HKU-UCAS Joint Institute of Theoretical and Computational Physics,*
The University of Hong Kong, Pokfulam Road, Hong Kong SAR, China
[2]*Department of Physics, University of Florida, Gainesville, Florida 32601, USA*
[3]*Department of Physics, University of Michigan, Ann Arbor, Michigan 48109, USA*

Novel critical phenomena beyond the Landau-Ginzburg-Wilson paradigm have been long sought after. Among many candidate scenarios, the deconfined quantum critical point (DQCP) constitutes the most fascinating one, and its lattice model realization has been debated over the past two decades. Here we apply the spherical Landau level regularization upon the exact $(2 + 1)$D SO(5) nonlinear sigma model with a topological term to study the potential DQCP therein. We perform a density matrix renormalization group (DMRG) simulation with $\mathrm{SU(2)_{spin} \times U(1)_{charge} \times U(1)_{angular-momentum}}$ symmetries explicitly implemented. Using crossing point analysis for the critical properties of the DMRG data, accompanied by quantum Monte Carlo simulations, we accurately obtain the comprehensive phase diagram of the model and find various novel quantum phases, including Néel, ferromagnet (FM), valence bond solid (VBS), valley polarized (VP) states and a gapless quantum disordered phase occupying an extended area of the phase diagram. The VBS-disorder and Néel-disorder transitions are continuous with non-Wilson-Fisher exponents. Our results show the VBS and Néel states are separated by either a weakly first-order transition or the disordered region with a multicritical point in between, thus opening up more interesting questions on the two-decade long debate on the nature of the DQCP.

Introduction.—Over the past two decades, the enigma of the deconfined quantum critical point (DQCP) has never failed to attract attention across the communities of condensed matter to quantum field theory and high-energy physics, as it is believed to offer a new paradigm in theory [1–5], numerical simulation [6–15], and experiment [16–21] that goes beyond the Landau-Ginzburg-Wilson (LGW) framework of phase transitions.

However, the lattice realizations of DQCP have been debated ever since. In SU(2) spin systems, the $J - Q$ model [6] was initially believed to realize a DQCP between Néel and valence bond solid (VBS) states. Over the years, a plethroa of results have been reported, including the emergent continuous symmetry with fractionalized excitations [12–15] yet drifting critical exponents incompatible with conformal bootstrap bounds [with one O(3) $\times \mathbb{Z}_4$ singlet] [2,8,11,22,23], weakly first-order pseudocriticality versus continuous transition or multicritical point [2,24–31], and violation of entanglement positivity for a unitary conformal field theory (CFT) [32–34]; and debate regarding the nature of the phase transition persists to this day. A more recent quantum Monte Carlo (QMC) study suggests the nonunitary CFT of the DQCP scenario in SU(N) spin systems for $N < N_c \simeq 8$ [35].

Similar changing perceptions also occur in DQCP models with fermions, realizing transitions from a Dirac semimetal (DSM) through quantum spin Hall insulator to superconductor [9,36,37], or from DSM through VBS to a Néel state [10,38,39]. The inclusion of fermions offers advantages over the previous model, due to the absence of symmetry-allowed quadruple monopoles and the associated second length scale that breaks the assumed U(1) symmetry down to $\mathbb{Z}_4$ [2,11], but the noncompatible critical exponents still persist and the accumulating numerical results are also pointing towards a nonunitary CFT of these DQCPs [9,10,34,36,39–41]. Despite extensive efforts over the past two decades, the lattice realizations of the DQCP in its original sense of beyond the LGW framework and yet still critical, with emergent continuous symmetry and fractionalized excitations, are still in "The Enigma of Arrival" [42].

A key origin of the debate stems from the fundamental requirement of emergent symmetries at DQCPs. For instance, the $J - Q$ model DQCP is speculated to have a U(1) symmetry emerge out of the $\mathbb{Z}_4$ symmetry of VBS, which is then speculated to be combined with the SU(2) symmetry of the Néel order to give rise to the ultimate SO(5) emergent symmetry. Because of the extremely slow RG flow towards such emergent symmetries, numerical studies face challenges in accessing these speculated DQCPs due to finite size effects. To overcome this challenge, lattice models with explicit SO(5) symmetry

have been introduced, e.g., the $(2+1)$D SO(5) nonlinear sigma model (NLSM) with a Wess-Zumino-Witten (WZW) topological term [43]. In such a model, different from the aforementioned $J-Q$ and fermion realizations, one can directly ask the question whether there is a continuous Néel-VBS transition in its phase diagram, without the hierarchy of symmetries emergence.

However, previous attempts for such a SO(5) model with the half-filled Landau level of Dirac fermions as a regularization on torus geometry, were unfortunately limited by severe computational complexity both for density matrix renormalization group (DMRG) and QMC simulations [41,44]. Moreover, these works have not addressed the entire phase diagram with control parameters moving away from the SO(5) symmetric path, such that the transitions towards the SO(3) symmetry-breaking Néel phase and the SO(2) symmetry-breaking VBS phase have not been addressed. Therefore, the results are still inconclusive and different scenarios—such as the first order transition between Néel and VBS phases, the multicritical point and the DQCP scenarios—are all suggested.

Here, we push forward the solution of the problem by applying the spherical Landau level regularization which was studied in the context of fractional quantum Hall effect in the early literature [45–48] and has recently been shown to suffer a less finite-size effect than the torus geometry for the $(2+1)$D Ising model [49]. To facilitate the large system sizes and quantitative data analysis, we perform a DMRG simulation with explicit $SU(2)_{spin} \times U(1)_{charge} \times U(1)_{angular-momentum}$ symmetries, accompanied with exact diagonalization (ED) and QMC simulations. We accurately simulate the entire phase diagram of the model with various novel quantum states identified, including the Néel, VBS, ferromagnet (FM), and valley polarized (VP) states. Most importantly, we find a gapless disordered region separates the VBS and Néel states. We employ the crossing point analysis [3,11,15,50,51] for the critical properties of the DMRG data and find the VBS-disorder and Néel-disorder transitions are continuous with non-Wilson-Fisher exponents. These critical boundaries meet at a multicritical point along the SO(5) line behind which the SO(5) symmetry is explicitly broken with a weakly first order transition between the Néel and VBS phases. Our results are supported by a recent conformal bootstrap analysis on the quantum tricriticality on the DQCP [52], as well as the QMC entanglement entropy results of the $J-Q$ model that at the Néel-VBS transition is weakly first order [53,54].

Our discovery of the extended gapless disordered phase and the multicritical point, and our novel methodology of the crossing point analysis of the DMRG data, open a few new research directions, such as the nature of the disordered phase, its relation with pseudocriticality and symmetry-enforced gaplessness [4], and its transition between VBS and Néel phases. These results substantially advance the two-decade long quest of the DQCP in the phase diagram of the $(2+1)$D SO(5) NLSM with a WZW topological term.

Model and methods.—We consider the $(2+1)$D Hamiltonian $H_\Gamma = \frac{1}{2}\int d\Omega\{U_0[\psi^\dagger(\Omega)\psi(\Omega)-2]^2 - \sum_{i=1}^5 u_i[\psi^\dagger(\Omega)\Gamma^i\psi(\Omega)]^2\}$, where $\psi_{\tau\sigma}(\Omega)$ is the four-component Dirac fermion annihilation operator with valley τ and spin σ indices, and $\Gamma^i = \{\tau_x \otimes \mathbb{I}, \tau_y \otimes \mathbb{I}, \tau_z \otimes \sigma_x, \tau_z \otimes \sigma_y, \tau_z \otimes \sigma_z\}$ are the five mutually anticommuting matrices, whose commutators $L^{ij} = -\frac{i}{2}[\Gamma^i, \Gamma^j]$ are generators of the SO(5) group. Subsequently, we project the Hamiltonian onto the zero energy Landau level on the sphere, which is the same as the lowest massive fermion Landau levels (LLLs) of a sphere with a $4\pi s$ magnetic monopole [55–57], where the $(2s+1)$-fold degenerate LLL wave functions are $\Phi_m(\Omega) \propto e^{im\phi}\cos^{s+m}(\theta/2)\sin^{s-m}(\theta/2)$ with $m \in \{-s, -s+1, \ldots, s\}$ and $2s \in \mathbb{Z}$. Via the expansion $\psi(\Omega) = \sum_m \Phi_m(\Omega)c_m$, we have

$$\hat{H}_\Gamma = U_0\hat{H}_0 - \sum_i u_i\hat{H}_i, \text{ with}$$

$$\hat{H}_i = \sum_{m_1,m_2,m} V_{m_1,m_2,m_2-m,m_1+m}$$
$$\times (c_{m_1}^\dagger\Gamma^i c_{m_1+m} - 2\delta_{i0}\delta_{m0})(c_{m_2}^\dagger\Gamma^i c_{m_2-m} - 2\delta_{i0}\delta_{m0}) \quad (1)$$

with $\Gamma^0 = \mathbb{I} \otimes \mathbb{I}$. The precise form of V_{m_1,m_2,m_3,m_4} can be found in the Supplemental Material (SM) [58]. Throughout, we set $U_0 = 1$ as the energy unit and let $u_1 = u_2 = u_K$, $u_3 = u_4 = u_5 = u_N$. When $u_K = u_N > 0$, this model is known to be described by a SO(5) NLSM with a WZW term [41,43,44]. When $u_K \neq u_N$, the symmetry reduces to SO(3) × SO(2). For positive $u_{K,N}$, it was proposed that $u_N > u_K$ stabilizes the Néel order, which spontaneously breaks the SO(3) symmetry, while $u_N < u_K$ favors a valley order breaking the SO(2) symmetry, which in a lattice model can be interpreted as the VBS order. We note, however, such an explicit perturbation away from the SO(5) symmetric path has not been investigated in previous studies. If a direct and continuous phase transition between these two states arises at $u_K = u_N$, at the transition the system has an explicit SO(5) symmetry, which realizes a DQCP. While previous works mainly focused on positive values for $u_{K,N}$ along the SO(5) line, we sweep the entire (u_K, u_N) plane for symmetry breaking phases.

We perform a DMRG simulation with $SU(2)_{spin} \times U(1)_{charge} \times U(1)_{angular-momentum}$ symmetries in the tensor library QSpace [62–64], and keep up to 4096 SU(2) invariant multiplets [equivalent to ∼12000 U(1) states] to render the truncation errors within 5×10^{-5}. We also perform determinant QMC as well as ED simulations as complements. We denote the system size by the Landau level degeneracy $N = 2s+1$ and obtain converging results up to $N = 16$, the largest size achieved so far for the model on a sphere, to our knowledge. To determine the VBS-disorder and

Néel-disorder critical points and the critical exponents in an unbiased manner, we adopt the crossing point analysis that has been used in earlier studies for many in quantum-critical spin models [3,11,15,50,51]. The derivation and detailed steps are given in the SM [58].

Phase diagram.—We first give a summary of the phase diagram. For all the ordered phases observed, the order parameters take the form of fermion bilinears: $\langle O \rangle = \int d\Omega \langle \psi^\dagger(\Omega) M \psi(\Omega) \rangle = \sum_m \langle c_m^\dagger M c_m \rangle$, where M
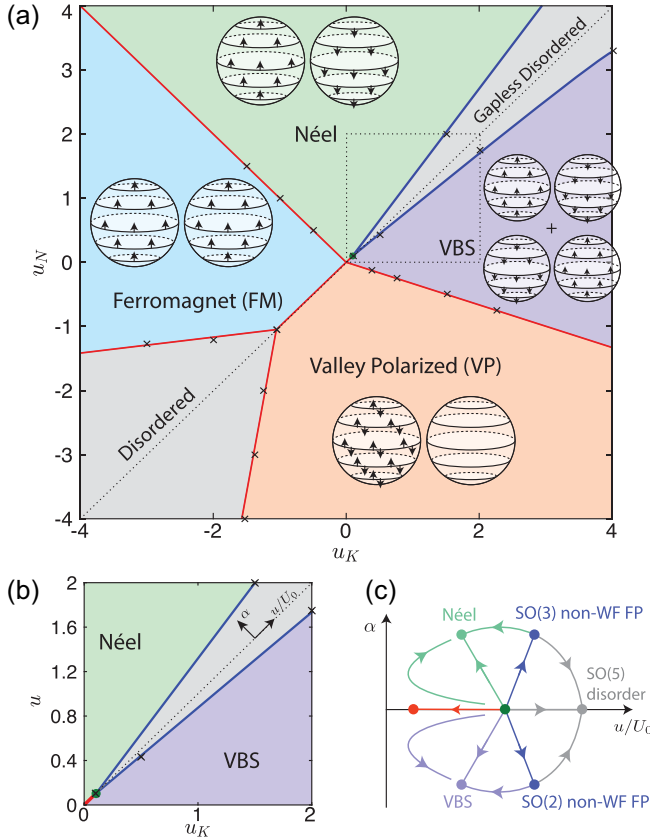
FIG. 1. The ground state phase diagram and RG flow of the SO(5) model. (a) Overall phase diagram with Néel, VBS, ferromagnet (FM), valley polarized (VP) phases, and the disorder phases as denoted. The deep blue lines denote the continuous and the non-Wilson-Fisher transition, the red lines denote the first-order transition, and the deep green dot denotes a multicritical point. The four symmetry-breaking states are schematically depicted by two spheres for the two opposite valleys, and the spin degrees of freedom are depicted by the arrow directions. (b) Enlarged phase diagram as indicated by the dashed box in panel (a). The two critical boundaries meet at a multicritical point (deep green dot) below which the SO(5) symmetry is spontaneously broken. (c) Possible RG flow in the considered parameter space in (b), with multicritical point (deep green dot), SO(5) disorder (grey dot), non-Wilson-Fisher fixed points (blue dots) towards SO(2) breaking VBS-ordered (light purple dot) and SO(3) breaking Néel-orderd (light green dot) fixed points, and the SO(5) breaking (red dot) fixed point. The α and u/U_0 axes are indicated in panel (b).

is either a Γ matrix or one of the SO(5) generators L^{ij}. In the case of $(u_K, u_N) > 0$, there are three phases including the Néel state (ordered in the $\Gamma^{3,4,5}$ directions), the VBS (ordered in the $\Gamma^{1,2}$ directions), and the disorder phase, as shown in Fig. 1. At small $u_{K,N}$ (below ~0.1), the Néel and VBS phases are separated by a first-order phase boundary, along the $u_K = u_N$ line with SO(5) symmetry. At large $u_{K,N}$, instead of the proposed direct and continuous transition, we find that Néel and VBS phases are separated by an intermediate disordered phase, and continuous transitions from the disordered state to both Néel and VBS states. (We will discuss the critical behavior of VBS-disorder and Néel-disorder transitions in the next section.)

For negative values of u_K and/or u_N, we find three phases: the FM state ($M = L^{34}, L^{35}, L^{45}$) where both valleys exhibit the same magnetization direction, the VP state ($M = L^{12}$) which breaks an Ising $\mathbb{Z}_2$ symmetry, and another disorder phase. When $|u_{K,N}|$ are small [i.e., $(u_K, u_N) > -1$], the FM and VP states are directly connected by a first-order transition along the SO(5) line. Again, for larger $|u_{K,N}|$, the FM and VP phases are separated by the disordered phase, while the transitions between the FM, VP, and disordered states are all first order.

The transition between the FM and Néel states takes place in the quadrant of $u_K < 0$ and $u_N > 0$ through a first order phase boundary. Similarly, a first-order transition between the VBS and VP states is observed in the quadrant of $u_K > 0$ and $u_N < 0$.

Phases of the $(u_K, u_N) > 0$ quadrant.—We first focus on the positive $u_{K,N}$ cases, and compute the squared order parameter $\langle O_i^2 \rangle$ with $O_i = \int d\Omega \psi^\dagger(\Omega)\Gamma^i \psi(\Omega) = \sum_m c_m^\dagger \Gamma^i c_m$. We use $m_{\text{Néel}}^2 = \frac{1}{3N^2}\langle (O_3^2 + O_4^2 + O_5^2) \rangle$ and $m_{\text{VBS}}^2 = \frac{1}{2N^2}\langle (O_1^2 + O_2^2) \rangle$ for Néel and VBS orders, respectively.

To systematically determine the VBS-Disorder transition, we fix a few $u_K = 0.5, 2, 4$ values and scan u_N. The representative $u_K = 2$ scan is shown in Fig. 2. Figure 2(a) shows the VBS Binder ratio $U_{\text{VBS}} \equiv \langle O_1^2 \rangle^2 / \langle O_1^4 \rangle$ crosses between the successive size pair $(N, N+1)$, it is clear that there is a crossing of the data which indicates the transition point. To locate the transition point in an unbiased manner, we employ the crossing point analysis as detailed in the SM [58] and find that the $u_N^* = u_c + N^{-(1/2\nu)-(\omega/2)}$ (the asterisk indicates the finite-size crossing points) nicely extrapolate to the $u_c = 1.75(4)$ with the correlation length exponent $\nu = 0.47(3)$ and subleading exponent $\omega = 2.2(4)$ independently obtained from Binder ratio $U^*(u_N^*, N) = a + bN^{-(\omega/2)}$ and its derivatives $\frac{1}{\nu^*} \equiv 2N \ln[(U'(u_N^*, N+1))/(U'(u_N^*, N))] = \frac{1}{\nu} - cN^{-(\omega/2)}$ at finite N, as shown in Fig. 2(b). With the obtained u_c and ν, one can further collapse the VBS order parameter as $m_{\text{VBS}}^2 \cdot N^{\Delta_{\text{VBS}}}$ against $\sqrt{N}^{1/\nu}(u_N - u_c)/u_c$ and unbiasedly obtain the scaling
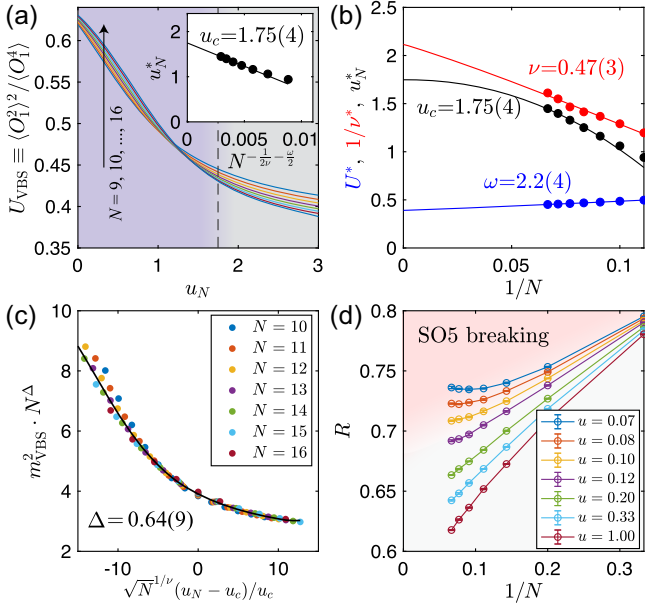
FIG. 2. Crossing point analysis of the VBS-disorder transitions. Along the fixed $u_K = 2$ cut, (a) the VBS Binder ratio $U_{\text{VBS}} \equiv \langle O_1^2 \rangle^2 / \langle O_1^4 \rangle$ crosses between successive size pair $(N, N+1)$, whose crossing points u_N^* drift towards larger u_N with larger N. In the inset, u_N^*'s are extrapolated to $u_c = 1.75(4)$ in the thermodynamic limit with the scaling form $u_N^*(N) = u_c + N^{-(1/2\nu)-(\omega/2)}$, with $\nu = 0.47(3)$ and $\omega = 2.2(4)$ from the crossing point analysis shown in the SM [58]. (b) The subleading operator exponent ω, correlation length exponent ν, and the critical point u_c are obtained from the scaling form of the crossing point, Binder ratio value at crossing point and its first-order derivatives. (c) m_{VBS}^2 rescaled by N^Δ with scaling dimension $\Delta = 0.64(9)$ versus $\sqrt{N}^{1/\nu}(u_N - u_c)/u_c$, collapses nicely for various system sizes $N = 9, 10, \ldots, 16$. (d) Correlation ratio R (up to $N = 15$), along the SO(5) line, indicates the phase transition point near $u \simeq 0.1$.

dimension $\Delta_{\text{VBS}} = 0.64(9)$, as shown in Fig. 2(c). We note the collapse is of very good quality and the obtained $\Delta_{\text{VBS}} = 0.64(9)$ is substantially larger than its O(2) Wilson-Fisher counterpart 0.519. This gives a clear signature, that the VBS-Disorder transition is not of Wilson-Fisher type and there is no direct VBS-Néel DQCP transition at $u_K = 2$. We have further performed the same analysis at $u_K = 0.5, 4$ and obtained an equally good and consistent critical point $u_c = 0.43(3), 3.3(2)$ and exponents $\nu = 0.55(5), 0.49(5)$, $\omega = 2.2(4), 2.1(1)$, and VBS scaling dimension $\Delta_{\text{VBS}} = 0.63(8)$, $0.63(9)$; the results are shown in the SM [58]. Similar simulations are performed with fixed the $u_N = 2$ cut and $u_c = 1.5(3), \Delta = 0.55(3)$ are found. With these data, we map out the phase boundaries of both VBS-Disorder and Néel-Disorder transitions as shown in Fig. 1(a). We find the continuous VBS-disorder and Néel-disorder transitions are merged into one multicritical point at $u_K = u_N \simeq 0.1$, as denoted in Fig. 1(b). For $u_K = u_N = u \lesssim 0.1$, the SO(5) line
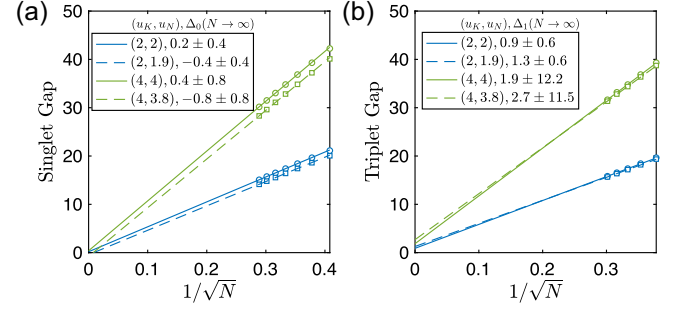
FIG. 3. Spin gaps within disordered phase. Within the disordered phase, (a) spin singlet gaps and (b) spin triplet gaps are calculated in the finite-size cases, and extrapolated to zero with $1/\sqrt{N}$ in the thermodynamic limit.

represents a first-order phase boundary with the SO(5) symmetry spontaneously broken.

To verify such a first-order line, we simulate along the exact SO(5) line $u_K = u_N = u$. As shown in Fig. 2(d), correlation ratios $R \equiv 1 - \langle O_{l=1}^2 \rangle / \langle O_{l=0}^2 \rangle$ for up to sizes $N = 15$, indicate the phase transition point near $u \simeq 0.1$. Here $\mathbf{O}_l \equiv (O_{1,l}, \ldots, O_{5,l})$ is the O(5) order parameter with angular momentum shift l [58]. Since the multicritical point is the meeting point of the SO(2)-breaking and SO(3)-breaking critical boundaries, it requires us to fine-tune two different control parameters, u_K and u_N, in order to access.

Within disordered phase, we calculate the spin-singlet gap $\Delta_0 = E_1(S = 0) - E_0(S = 0)$ and triplet gap $\Delta_1 = E_0(S = 1) - E_0(S = 0)$, with $E_i(S)$ the ith lowest energy in the total spin-S sector. In Fig. 3, both kinds of gaps follow a clear $1/\sqrt{N}$ behavior and scale to zero in the thermodynamic limit. Such a scaling behavior of the gaps strongly implies the disordered phase is gapless, fully consistent with the symmetry-enforced gaplessness discussed in Ref. [4].

Phases of the $(u_K, u_N) < 0$ quadrant.—For negative u_K and u_N, the order parameter with $M = \Gamma^i$ vanishes in the thermodynamic limit. Instead, the relevant order parameter involves the SO(5) generator $M = L^{ij}$. We calculate the squared generators $\langle \tilde{O}_{ij}^2 \rangle$ with $\tilde{O}_{ij} = \int d\Omega \psi^\dagger(\Omega) L^{ij} \psi(\Omega) = \sum_m c_m^\dagger L^{ij} c_m$, and define the squared FM order parameter as $m_{\text{FM}}^2 = \frac{1}{N^2} \langle (\tilde{O}_{34}^2 + \tilde{O}_{35}^2 + \tilde{O}_{45}^2) \rangle$, and the squared VP order parameter as $m_{\text{VP}}^2 = \frac{1}{N^2} \langle \tilde{O}_{12}^2 \rangle$. As $L^{12} = \tau_z$, $L^{34} = -\sigma_z$, $L^{35} = \sigma_y$, $L^{45} = \sigma_x$, the finite value of m_{VP}^2 and m_{FM}^2 suggests the VP and FM states, respectively.

In Figs. 4(a) and 4(b), we simulate along the negative SO(5) line $u_K = u_N = u < 0$. The ground state energies $e_g = \frac{1}{N} \langle \psi | H_\Gamma | \psi \rangle$ show clear kinks at $u_c(N)$ which can be extrapolated to $u_c(\infty) \simeq -1.056$ (c.f. the inset). As shown in Fig. 4(b), such a first-order transition can also be seen from the squared order parameter $\langle \tilde{O}^2 \rangle / N^2$, which rapidly jumps from zero to a finite plateau, whose height decreases upon increasing N and can be extrapolated to the value of 4.
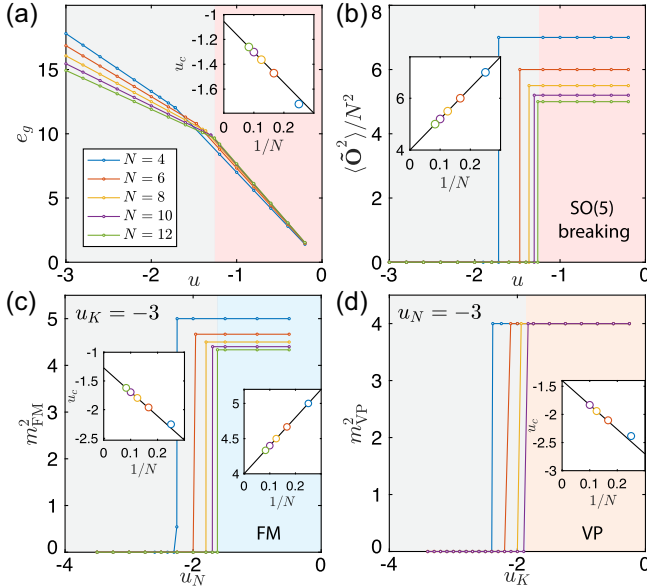
FIG. 4. Identification of the FM and VP phases. Along the negative SO(5) line $u_N = u_K = u$, (a) the ground state energy e_g exhibits kinks around $u \sim -1$. In the inset, the kink position $u_c(N)$ is extrapolated to $u_c(\infty) \simeq -1.056$. (b) $\langle \tilde{\mathbf{O}}^2 \rangle / N^2$ shows a sudden jump around u_c. (c) Along a fixed $u_K = -3$ line, m_{FM}^2 shows a sudden jump behavior. In the left inset, the transition points are extrapolated linearly to $u_c(\infty) \simeq -1.25$. (d) Along a fixed $u_N = -3$ line, m_{VP}^2 shows a sudden jump behavior. In the inset, the transition points are extrapolated linearly to $u_c(\infty) \simeq -1.38$.

In Fig. 4(c), we further determine the $u_K = -3$ cut in the phase diagram. The value of m_{FM}^2 jumps from zero to finite around $u_N(N = \infty) \simeq -1.25$. Similarly in Fig. 4(d), we simulate the fixed $u_N = -3$ cut where m_{VP}^2 jumps to a finite value of four around $u_K(N = \infty) \simeq -1.38$. More DMRG results concerning the first-order transitions between VP and VBS, and between FM and Néel phases, are shown in the SM [58].

Discussions.—Our study provides a comprehensive phase diagram for the $(2+1)$D SO(5) NLSM with a WZW term on a sphere. It reveals novel quantum states and suggests a SO(5) disordered region separating the SO(2) breaking VBS and SO(3) breaking Néel phases, which terminates at a multicritical point [27]. Our discovery of the extended disordered phase and the multicritical point using a novel method of crossing point analysis of the DMRG data, may also offer a platform for the search of the predicted pseudocritical behavior [4], which we leave for future studies. These results, combined with recent observations of a weakly first-order transition from entanglement measurements [32–36,39,53,54] as well as the conformal bootstrap deconfined quantum tricriticality [52], open up new directions for the two-decade long pursuit of the DQCP in various Néel-to-VBS settings.

Furthermore, our results find resonance with the experiments both in the VBS-AFM transition in the quantum magnet SrCu$_2$(BO$_3$)$_2$ [16–18,20,21] and the QSH-SC transition in monolayer WTe$_2$ [65], where the systems either exhibit a first order transition or an intermediate phase. A new pathway towards a conformal 2D SU(2) DQCP was recently proposed, with $\mathrm{SO}(5)_f \times \mathrm{SO}(5)_b$ global symmetry [66]. Investigating the validity of this newly proposed DQCP using present techniques would be of great interest.

Note added.—Recently, Ref. [67] reported pseudocritical behavior for the SO(5) line. The parameter range of the reported pseudocritical behavior and (approximate) conformal symmetry, i.e., $0.7 < V/U < 1.5$, correspond to $0.1187 < u/U_0 < 0.4286$, close to the multicritical point in our phase diagram.

* yuxuan.wang@ufl.edu
† sunkai@umich.edu
‡ zymeng@hku.hk

[1] T. Senthil, L. Balents, S. Sachdev, A. Vishwanath, and M. P. A. Fisher, Phys. Rev. B **70**, 144407 (2004).

[2] A. Nahum, J. T. Chalker, P. Serna, M. Ortuño, and A. M. Somoza, Phys. Rev. X **5**, 041048 (2015).

[3] Y. Q. Qin, Y.-Y. He, Y.-Z. You, Z.-Y. Lu, A. Sen, A. W. Sandvik, C. Xu, and Z. Y. Meng, Phys. Rev. X **7**, 031052 (2017).

[4] C. Wang, A. Nahum, M. A. Metlitski, C. Xu, and T. Senthil, Phys. Rev. X **7**, 031051 (2017).

[5] T. Senthil, arXiv:2306.12638.

[6] A. W. Sandvik, Phys. Rev. Lett. **98**, 227202 (2007).

[7] J. Lou, A. W. Sandvik, and N. Kawashima, Phys. Rev. B **80**, 180414(R) (2009).

[8] K. Harada, T. Suzuki, T. Okubo, H. Matsuo, J. Lou, H. Watanabe, S. Todo, and N. Kawashima, Phys. Rev. B **88**, 220408(R) (2013).

[9] Y. Liu, Z. Wang, T. Sato, M. Hohenadler, C. Wang, W. Guo, and F. F. Assaad, Nat. Commun. **10**, 2658 (2019).

[10] Y. Da Liao, X. Y. Xu, Z. Y. Meng, and Y. Qi, Phys. Rev. B **106**, 075111 (2022).

[11] H. Shao, W. Guo, and A. W. Sandvik, Science **352**, 213 (2016).

[12] N. Ma, G.-Y. Sun, Y.-Z. You, C. Xu, A. Vishwanath, A. W. Sandvik, and Z. Y. Meng, Phys. Rev. B **98**, 174421 (2018).

[13] A. Nahum, P. Serna, J. T. Chalker, M. Ortuño, and A. M. Somoza, Phys. Rev. Lett. **115**, 267203 (2015).

[14] G. J. Sreejith, S. Powell, and A. Nahum, Phys. Rev. Lett. **122**, 080601 (2019).

[15] N. Ma, Y.-Z. You, and Z. Y. Meng, Phys. Rev. Lett. **122**, 175701 (2019).

[16] J. L. Jiménez, S. P. G. Crone, E. Fogh, M. E. Zayed, R. Lortz, E. Pomjakushina, K. Conder, A. M. Läuchli, L. Weber, S. Wessel, A. Honecker, B. Normand, Ch. Rüegg, P. Corboz, H. M. Rønnow, and F. Mila, Nature (London) **592**, 370 (2021).

[17] M. E. Zayed, Ch. Rüegg, J. Larrea J., A. M. Läuchli, C. Panagopoulos, S. S. Saxena, M. Ellerby, D. F. McMorrow, Th. Strässle, S. Klotz, G. Hamel, R. A. Sadykov, V. Pomjakushin, M. Boehm, M. Jiménez–Ruiz, A. Schneidewind, E. Pomjakushina, M. Stingaciu, K. Conder, and H. M. Rønnow, Nat. Phys. **13**, 962 (2017).

[18] J. Guo, G. Sun, B. Zhao, L. Wang, W. Hong, V. A. Sidorov, N. Ma, Q. Wu, S. Li, Z. Y. Meng, A. W. Sandvik, and L. Sun, Phys. Rev. Lett. **124**, 206602 (2020).

[19] G. Sun, N. Ma, B. Zhao, A. W. Sandvik, and Z. Y. Meng, Chin. Phys. B **30**, 067505 (2021).

[20] Y. Cui, L. Liu, H. Lin, K.-H. Wu, W. Hong, X. Liu, C. Li, Z. Hu, N. Xi, S. Li, R. Yu, A. W. Sandvik, and W. Yu, Science **380**, 1179 (2023).

[21] J. Guo, P. Wang, C. Huang, B.-B. Chen, W. Hong, S. Cai, J. Zhao, J. Han, X. Chen, Y. Zhou, S. Li, Q. Wu, Z. Y. Meng, and L. Sun, arXiv:2310.20128.

[22] Y. Nakayama and T. Ohtsuki, Phys. Rev. Lett. **117**, 131601 (2016).

[23] D. Poland, S. Rychkov, and A. Vichi, Rev. Mod. Phys. **91**, 015002 (2019).

[24] A. B. Kuklov, M. Matsumoto, N. V. Prokof'ev, B. V. Svistunov, and M. Troyer, Phys. Rev. Lett. **101**, 050405 (2008).

[25] F.-J. Jiang, M. Nyfeler, S. Chandrasekharan, and U.-J. Wiese, J. Stat. Mech. (2008) P02009.

[26] K. Chen, Y. Huang, Y. Deng, A. B. Kuklov, N. V. Prokof'ev, and B. V. Svistunov, Phys. Rev. Lett. **110**, 185701 (2013).

[27] B. Zhao, J. Takahashi, and A. W. Sandvik, Phys. Rev. Lett. **125**, 257204 (2020).

[28] J. D'Emidio, A. A. Eberharter, and A. M. Läuchli, SciPost Phys. **15**, 061 (2023).

[29] R. Ma and C. Wang, Phys. Rev. B **102**, 020407(R) (2020).

[30] A. Nahum, Phys. Rev. B **102**, 201116(R) (2020).

[31] A. W. Sandvik and B. Zhao, Chin. Phys. Lett. **37**, 057502 (2020).

[32] J. Zhao, Y.-C. Wang, Z. Yan, M. Cheng, and Z. Y. Meng, Phys. Rev. Lett. **128**, 010601 (2022).

[33] Y.-C. Wang, N. Ma, M. Cheng, and Z. Y. Meng, SciPost Phys. **13**, 123 (2022).

[34] Z. H. Liu, Y. Da Liao, G. Pan, M. Song, J. Zhao, W. Jiang, C.-M. Jian, Y.-Z. You, F. F. Assaad, Z. Y. Meng, and C. Xu, Phys. Rev. Lett. **132**, 156503 (2024).

[35] M. Song, J. Zhao, M. Cheng, C. Xu, M. M. Scherer, L. Janssen, and Z. Y. Meng, arXiv:2307.02547.

[36] Z. H. Liu, W. Jiang, B.-B. Chen, J. Rong, M. Cheng, K. Sun, Z. Y. Meng, and F. F. Assaad, Phys. Rev. Lett. **130**, 266501 (2023).

[37] Z. H. Liu, M. Vojta, F. F. Assaad, and L. Janssen, Phys. Rev. Lett. **128**, 087201 (2022).

[38] Y. Da Liao, X. Y. Xu, Z. Y. Meng, and Y. Qi, Phys. Rev. B **106**, 155159 (2022).

[39] Y. Da Liao, G. Pan, W. Jiang, Y. Qi, and Z. Y. Meng, arXiv:2302.11742.

[40] Z. Wang, Y. Liu, T. Sato, M. Hohenadler, C. Wang, W. Guo, and F. F. Assaad, Phys. Rev. Lett. **126**, 205701 (2021).

[41] Z. Wang, M. P. Zaletel, R. S. K. Mong, and F. F. Assaad, Phys. Rev. Lett. **126**, 045701 (2021).

[42] V. Naipaul, The Enigma of Arrival: A Novel in Five Sections, Picador Classic (Pan Macmillan, London, 2020).

[43] J. Lee and S. Sachdev, Phys. Rev. Lett. **114**, 226801 (2015).

[44] M. Ippoliti, R. S. K. Mong, F. F. Assaad, and M. P. Zaletel, Phys. Rev. B **98**, 235108 (2018).

[45] F. D. M. Haldane, Phys. Rev. Lett. **51**, 605 (1983).

[46] S. L. Sondhi, A. Karlhede, S. A. Kivelson, and E. H. Rezayi, Phys. Rev. B **47**, 16419 (1993).

[47] V. Melik-Alaverdian, N. E. Bonesteel, and G. Ortiz, Phys. Rev. Lett. **79**, 5286 (1997).

[48] J. Zhao, D. N. Sheng, and F. D. M. Haldane, Phys. Rev. B **83**, 195135 (2011).

[49] W. Zhu, C. Han, E. Huffman, J. S. Hofmann, and Y.-C. He, Phys. Rev. X **13**, 021009 (2023).

[50] J. M. Luck, Phys. Rev. B **31**, 3069 (1985).

[51] N. Ma, P. Weinberg, H. Shao, W. Guo, D.-X. Yao, and A. W. Sandvik, Phys. Rev. Lett. **121**, 117202 (2018).

[52] S. M. Chester and N. Su, Phys. Rev. Lett. **132**, 111601 (2024).

[53] M. Song, J. Zhao, Z. Y. Meng, C. Xu, and M. Cheng, arXiv:2312.13498.

[54] Z. Deng, L. Liu, W. Guo, and H.-q. Lin, arXiv:2401.12838.

[55] A. Jellal, Nucl. Phys. **B804**, 361 (2008).

[56] M. Arciniaga and M. R. Peterson, Phys. Rev. B **94**, 035105 (2016).

[57] M. Greiter and R. Thomale, Ann. Phys. (Amsterdam) **394**, 33 (2018).

[58] See Supplemental Material at http://link.aps.org/supplemental/10.1103/PhysRevLett.132.246503, which includes Refs. [59–61], for additional information about the spherical Landau level regularization of the SO(5) model, detailed implementation in DMRG and QMC simulations, the crossing point analysis of the VBS-Disorder and Néel-Disorder non-Wilson-Fisher phase transitions and representative data.

[59] J. E. Hirsch, Phys. Rev. B **31**, 4403 (1985).

[60] X. Zhang, G. Pan, Y. Zhang, J. Kang, and Z. Y. Meng, Chin. Phys. Lett. **38**, 077305 (2021).

[61] X. Zhang, G. Pan, B.-B. Chen, H. Li, K. Sun, and Z. Y. Meng, Phys. Rev. B **107**, L241105 (2023).

[62] A. Weichselbaum, Ann. Phys. (Amsterdam) **327**, 2972 (2012).

[63] A. Weichselbaum, Phys. Rev. Res. **2**, 023385 (2020).

[64] B. Bruognolo, J.-W. Li, J. von Delft, and A. Weichselbaum, SciPost Phys. Lect. Notes, 25 (2021).

[65] T. Song, Y. Jia, G. Yu, Y. Tang, P. Wang, R. Singha, X. Gui, A. J. Uzan, M. Onyszczak, K. Watanabe, T. Taniguchi, R. J. Cava, L. M. Schoop, N. P. Ong, and S. Wu, Nat. Phys. **20**, 269 (2024).

[66] M. Christos, Z.-X. Luo, H. Shackleton, Y.-H. Zhang, M. S. Scheurer, and S. Sachdev, Proc. Natl. Acad. Sci. U.S.A. **120**, e2302701120 (2023).

[67] Z. Zhou, L. Hu, W. Zhu, and Y.-C. He, arXiv:2306.16435 [Phys. Rev. X (to be published)].

[68] https://cloud.paratera.com